

Expression of Human Carbonic Anhydrase in the Cyanobacterium *Synechococcus* PCC7942 Creates a High CO₂-Requiring Phenotype¹

Evidence for a Central Role for Carboxysomes in the CO₂ Concentrating Mechanism

G. D. Price and M. R. Badger*

Plant Environmental Biology Group, Research School of Biological Sciences, Australian National University,
P.O. Box 475, Canberra, A.C.T. 2601 Australia

ABSTRACT

Active human carbonic anhydrase II (HCAII) protein was expressed in the cyanobacterium *Synechococcus* PCC7942 by means of transformation with the bidirectional expression vector, pCA. This expression was driven by the bacterial *Tac* promoter and was regulated by the *lacI*Q repressor protein, which was expressed from the same plasmid. Expression levels reached values of around 0.3% of total cell protein and this protein appeared to be entirely soluble in nature and located within the cytosol of the cell. The expression of this protein has dramatic effects on the photosynthetic physiology of the cell. Induction of expression of carbonic anhydrase (CA) activity in both high dissolved inorganic carbon (C_i) and low C_i grown cells leads the creation of a high C_i requiring phenotype causing: (a) a dramatic increase in the K_{0.5} (C_i) for photosynthesis, (b) a loss of the ability to accumulate internal C_i, and (c) a decrease in the lag between the initial C_i accumulation following illumination and the efflux of CO₂ from the cells. In addition, the effects of the expressed CA can largely be reversed by the carbonic anhydrase inhibitor ethoxzolamide. As a result of the above findings, it is concluded that the CO₂ concentrating mechanism in *Synechococcus* PCC7942 is largely dependent on (a) the absence of CA activity from the cytosol, and (b) the specific localization of CA activity in the carboxysome. A theoretical model of photosynthesis and C_i accumulation is developed in which the carboxysome plays a central role as both the site of CO₂ generation from HCO₃⁻ and a resistance barrier to CO₂ efflux from the cell. There is good qualitative agreement between this model and the measured physiological effects of expressed cytosolic CA in *Synechococcus* cells.

inorganic carbon (C_i)² transport system. This system operates to elevate the intracellular concentration of CO₂ so that the relatively low affinity cyanobacterial Rubisco may function at close to CO₂ saturation. Models of this CO₂ concentrating mechanism have defined four key operational elements. These are: a transport system, a means to energize this using photosynthesis, a leak barrier to reduce the back flux of CO₂, and a mechanism to rapidly interconvert inorganic carbon species within the cell (1). The need to increase the rate of interconversion of C_i species is borne largely from evidence which suggests that the C_i transport system delivers HCO₃⁻ to the cytosol while Rubisco requires CO₂ as a substrate. The uncatalyzed conversion of HCO₃⁻ to CO₂ would be far too slow to support the observed rate of photosynthesis (3).

The interconversion of inorganic carbon species within the cell is mediated by the enzyme carbonic anhydrase. Theoretical models of the CO₂ concentrating mechanism have postulated two possible roles and intracellular locations for carbonic anhydrase, depending on the mechanistic assumptions which are made about the nature of the CO₂ leak barrier. If the barrier to CO₂ escape is associated with the cell membrane, then it is reasonable to assume that carbonic anhydrase will be located in the cytosol. In this case, Rubisco is assumed to be located either in the cytosol or the carboxysome, and would be freely accessible to CO₂. An alternative and more novel model proposes that the barrier to CO₂ leakage from the region of elevated CO₂ concentration may be the carboxysome protein coat (15). In this case, the carboxysome coat is assumed to be relatively permeable to HCO₃⁻ and relatively impermeable to CO₂. This protein coat would represent the primary barrier to CO₂ efflux from the site of carboxylation. With carbonic anhydrase localized exclusively within the carboxysome, a theoretical model can be used to calculate that CO₂ may be elevated within the confined internal space of the carboxysome (15). This model assumes that the cell

In cyanobacteria, the affinity of photosynthesis for external inorganic carbon is regulated by the presence of an active

¹ This work was supported by a National Research Fellowship (G. D. P.) awarded by the Australian Department of Education Employment and Training.

² Abbreviations: C_i, dissolved inorganic carbon; BTP, 1,3-bis[tris-(hydroxymethyl)methylamino]propane; CA, carbonic anhydrase; EPPS, *N*-(2-hydroxyethyl)piperazine-*N'*-3-propanesulfonic acid; EZ, ethoxzolamide; Rubisco, ribulose biphosphate carboxylase-oxygenase (EC 4.1.1.39); TES, *N*-tris(hydroxymethyl)methyl-2-aminoethanesulfonic acid; IPTG, isopropyl-β-D-thiogalactopyranoside.

membrane is relatively permeable to CO₂ diffusion. If this is the case, then some barrier must exist to prevent the efflux of C_i from the cytosol as CO₂. If C_i species are delivered to the cytosol as HCO₃⁻, then the obvious barrier would be the absence of carbonic anhydrase from this region, thus reducing the generation of CO₂ from HCO₃⁻ to the relatively slow uncatalyzed rate.

We have recently described the carbonic anhydrase activity associated with *Synechococcus* PCC7942 (2). Although this CA activity appears to be relatively low, the levels would appear to be sufficient to allow either of the above models to function effectively. Experiments aimed at localizing this CA activity to a particular compartment were able to show that some of the activity was associated with a pelletable fraction and this fraction contained both Rubisco activity and carboxysomes. Thus, the evidence to date is consistent with a carboxysomal location of CA activity.

A simple way to test whether there may be a strict requirement for CA activity to be localized within the carboxysome is to raise the level of CA activity within the cytosol and examine its subsequent effects on the ability to concentrate CO₂. If the second model were correct, then the expression of CA in the cytosol should cause the cytosolic inorganic carbon pool to be dissipated. This would be due to an increase in the rate of conversion of HCO₃⁻ to CO₂ which would subsequently lead to C_i loss by rapid leakage of CO₂ through the relatively permeable external membrane. On the other hand, the effect of cytosolic CA on C_i accumulation, as described by the first model, would not be expected to be significant.

This paper explores the result of such an experiment, where we have been able to express active human CAII protein within *Synechococcus* PCC7942 cells by means of a bidirectional expression plasmid. The results show quite clearly that this has the effect of eliminating the accumulation of C_i, increasing the leak rate of C_i out of the cell, and creating a high-CO₂-requiring phenotype. These results provide strong evidence that the carboxysome plays a central role in the CO₂ concentrating mechanism.

MATERIALS AND METHODS

Growth of Cyanobacteria

Synechococcus PCC7942 was grown in BG11 media (17) buffered to pH 8 with 10 mM BTP-HCl and gassed with 1% CO₂, 3% CO₂, or 30 μl · l⁻¹ CO₂ in air, as previously described (12, 13). Cyanobacteria carrying chloramphenicol resistance plasmids were grown in the presence of 10 μg · mL⁻¹ chloramphenicol in liquid.

Plate colonies were grown on 1% agar/BG11 buffered with 50 mM TES-KOH and containing 5 mM sodium thiosulphate (TTES plates) as previously described (13).

Preparation of Cells for Assays

Aliquots of cells were taken from the growth medium and harvested by centrifugation (4000g for 5 min at 25°C) and resuspended in CO₂-free growth medium at pH 8.0. Cells were kept in the dark at room temperature prior to their use.

Vectors and Strains

Plasmid pHCAII (a gift of B-H. Jonsson and S. Lindskog) is an *Escherichia coli* expression vector for human CAII (7). This plasmid contains a *tac* promoter (*lac/trp* hybrid) and a consensus *E. coli* ribosome binding site upstream of the HCAII gene. It also contains the *lac* repressor overproducing gene, *lacI*Q, to keep the *tac* promoter in a repressed state until the inducer IPTG is added to the growth media. Plasmid pHCAII also carries ampicillin resistance.

E. coli/Synechococcus shuttle vector pSK6B (GD Price, MR Badger, S Kirby, unpublished data) contains a 5.1 kb BamHI/BamHI fragment from the bidirectional shuttle vector, pVAD1 (6), ligated into the BamHI site of plasmid pUC18 (21). This 5.1 kb fragment carries a chloramphenicol resistance gene (chloramphenicol acetyl transferase; CAT) driven by the *psbA* chloroplast promoter and also contains the *Synechococcus* PCC7942 origin of replication from the small 7.9 kb endogenous plasmid.

E. coli HB101 (RecA-) was used as the host for the plasmids mentioned above. The following antibiotic concentrations were used with standard growth media (10) for selection of plasmids in *E. coli*: chloramphenicol, 25 μg · mL⁻¹; ampicillin, 25 μg · mL⁻¹.

Construction of *Synechococcus* Expression Vector for HCAII

The 5.1 kb BamHI fragment from plasmid pSK6B was ligated into the BglIII site in the plasmid pHCAII (Fig. 1). This produced a 9.6 kb *E. coli/Synechococcus* shuttle vector, plasmid pCA. DNA manipulations were carried out as described in Maniatis *et al.* (10). Plasmid DNA was transformed into *Synechococcus* PCC7942 by the method of Golden *et al.* (8) except that transformants were plated directly onto TTES plates containing 8 μg · mL⁻¹ chloramphenicol, and incubated at 1% CO₂ in air.

¹⁸O Exchange Kinetics of Cells

These were performed as described in the accompanying paper (14). Assays were done in a 2 mL volume at 30°C with a NaH¹³C¹⁸O₃ concentration of 1 mM for 1% CO₂-grown cells and 0.1 mM for 30 ppm-grown cells. The atom percent enrichment in doubly labelled CO₂ (mass 49) was calculated as:

$$\frac{(^{13}\text{C}^{18}\text{O}^{18}\text{O})}{(^{13}\text{CO}_2)} = \frac{(49)}{(45 + 47 + 49)}$$

C_i Accumulation Measurements

These were performed as previously described (3, 14). Cells were suspended in 2 mL of CO₂ free growth medium plus 20 mM Tes (pH 8.0) and placed in the cuvette at 30°C and bovine carbonic anhydrase (0.1 mg · mL⁻¹) was added. NaHCO₃ was added at either 1 mM (1% CO₂-grown cells) or 0.1 mM (30 ppm-grown cells) and the mass 44 signal was monitored. A calibration for C_i was made by injecting known amounts of

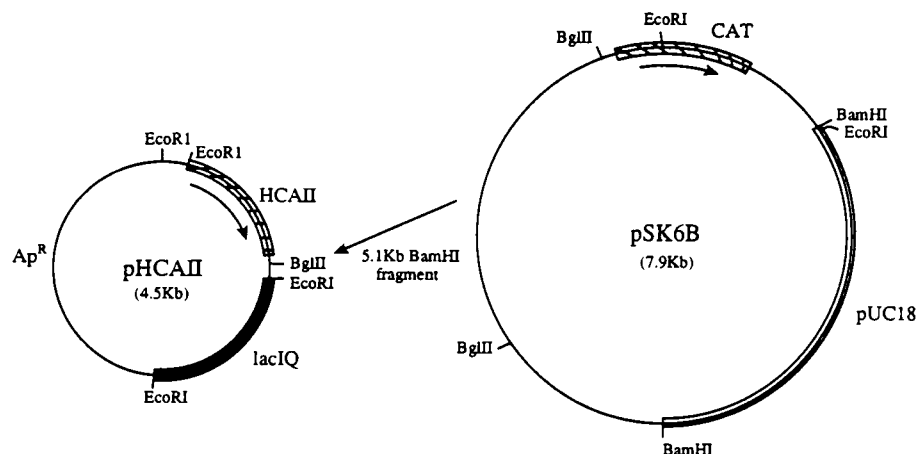


Figure 1. Strategy for the construction of the pCA bidirectional expression vector.

NaHCO₃ into the cuvette. Internal cell volume was assumed to be 60 $\mu\text{L} \cdot \text{mg}^{-1}$ Chl.

O₂-Electrode Measurements

These were made as previously described (12).

Carbonic Anhydrase Activity

Crude homogenates of cells were prepared as previously described (2), except that the extraction buffer was 100 mM EPPS-NaOH (pH 8.0), 10 mM MgSO₄, 1 mM EDTA, 0.5 mM PMSF, 10 μM leupeptin (Boehringer Mannheim), 10 mM DTT, and 10 $\mu\text{g} \cdot \text{mL}^{-1}$ DNase. Extracts were prepared in 1.2 mL of extraction buffer at Chl concentration of 150 to 300 $\mu\text{g} \cdot \text{mL}^{-1}$.

CA activity (as the CO₂ hydration activity) was measured at 0°C by the electrometric method of Wilbur and Anderson (19) using 3 mL of 5 mM EPPS (pH 8.2) as the assay buffer. A total of 200 μL of extraction buffer, including 25 to 50 μL of crude extract, was added to the assay. The reaction was initiated by the addition of 1.1 mL of ice-cold saturated H₂O and the time for the decrease in pH from 8.0 to 7.0 was recorded. Control assays were run with extracts prepared from cells containing the pSK6B plasmid. Enzyme activity was calculated as:

$$\text{Enzyme units} = 10 \left(\frac{T_b}{T_c} - 1 \right) / \text{mg Chl}$$

where T_b is the time for the uncatalysed reaction (control) and T_c is the time for the enzyme catalysed reaction. T_b was normally 90 to 92 s and T_c varied from 15 to 70 s.

The degree of pelletability of HCAII activity in crude extracts was measured by centrifugation of crude extracts in an Eppendorf centrifuge for 5 min at 10,000g (4°C). The pellet was resuspended in extraction buffer to the original volume. CA activity in the supernatant and pellet fractions was determined by the above method.

Protein Measurements

Protein was determined in crude extracts by using the Pierce protein assay kit (Pierce Chemical Co., Rockford, IL).

Chl Measurements

Chl was determined by the method of Wintermans and de Motts (20).

A Model of Photosynthesis and C_i Relationships

A steady state model of the relationships between C_i fluxes, pool sizes, and photosynthesis was constructed using the steady state equations developed by Reinhold *et al.* (15). These equations were used to solve for the cytosolic and carboxysomal concentrations of HCO₃⁻, CO₂, and photosynthesis. The estimates of the physical properties of the cells were as follows: cytoplasmic volume = $1.9 \times 10^{-12} \text{ cm}^3 \cdot \text{cell}^{-1}$; carboxysomal volume = $4.2 \times 10^{-14} \text{ cm}^3 \cdot \text{cell}^{-1}$; cell membrane area = $7.3 \times 10^{-8} \text{ cm}^2 \cdot \text{cell}^{-1}$; carboxysomal shell area = $12.7 \times 10^{-9} \text{ cm}^2 \cdot \text{cell}^{-1}$; V_{max} Rubisco = $2.6 \times 10^{-12} \mu\text{mol} \cdot \text{cell}^{-1} \cdot \text{s}^{-1}$; $K_{0.5}$ (CO₂) Rubisco = 150 μM (1); V_{max} C_i transport = 3.9 and $5.2 \times 10^{-12} \mu\text{mol} \cdot \text{cell}^{-1} \cdot \text{s}^{-1}$ for high and low C_i cells, respectively; $K_{0.5}$ (C_i) transport = 0.25 mM and 0.02 mM for high and low C_i cells respectively. The surface area and volume of the carboxysomes were calculated assuming them to be spheres of 200 nm diameter and that there were 10 carboxysomes per cell. For the purposes of the calculations presented here, the conductances of the cell membrane and carboxysomal shell were assumed to be 10^{-2} and $10^{-5} \text{ cm} \cdot \text{s}^{-1}$ for CO₂ and 10^{-6} and $10^{-4} \text{ cm} \cdot \text{s}^{-1}$ for HCO₃⁻ across the two respective membranes. These conductances are those shown to be effective in the *Anabaena* model of Reinhold *et al.* (15) and also appear to be appropriate for this *Synechococcus* model. The external pH was set at 8.0 while the internal pH of the cytosol and the carboxysome was assumed to be 7.6.

RESULTS

Expression of Carbonic Anhydrase

Figure 2 shows the level of carbonic anhydrase activity in 1% CO₂-grown pCA cells both before and after induction of expression with 0.5 mM IPTG. The CA activity prior to the addition of IPTG was in the range of 150 to 400 units $\cdot \text{mg Chl}^{-1}$, which is well above the almost undetectable level of CA present in wild type R2 or pSK6B cells grown under the same conditions (2). This indicates that even though the *lacIQ*

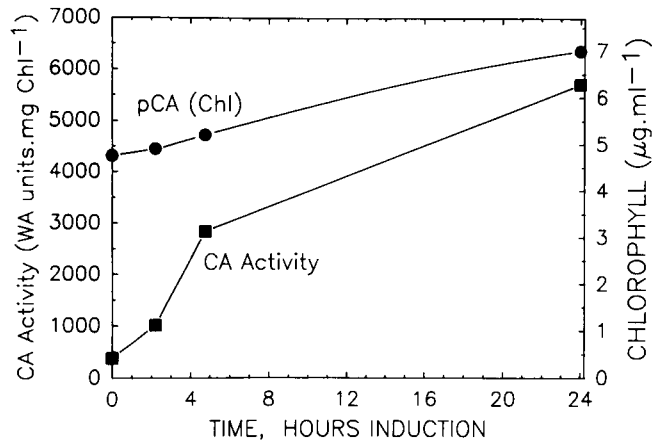


Figure 2. Induction of expression of CA activity following the addition of IPTG (0.5 mM) to pCA cells grown at 1% CO₂. The changes in CA activity (■) and the increase in the Chl concentration (●) of the growth medium are shown.

repressor gene is present on the plasmid, it does not keep the HCAII gene in a fully repressed state. Despite this, however, there is a dramatic increase in the CA activity after the addition of IPTG to the growth medium. Over a period of 24 h the level of CA rises to around 5000 units·mg Chl⁻¹. During this period there has been growth of the culture as indicated by the rise in Chl concentration. Assuming a specific activity of HCAII protein to be 60,000 units·mg protein⁻¹ under the assay conditions employed (16), the expression of CA after 24 h is about 0.3% of total cell protein.

Cellular Location of Expressed Carbonic Anhydrase

Establishing a cytosolic location of the expressed CA is important to interpreting the effects of this activity on cell physiology. It would normally be expected that an expressed protein, such as carbonic anhydrase in this instance, would be present as a soluble protein within the cytosol, unless some solubility problems are encountered. Measurements of pelletability (see "Materials and Methods") show that greater than 95% of the activity appears to be soluble in nature. Under these same extraction procedures, greater than 90% of the Rubisco activity and most of the endogenous CA activity are pelletable in nature (2). This indicates that the expressed CA does not form the same associations with cellular components such as thylakoids and carboxysomes that these native proteins do.

Effect of CA Expression on Photosynthetic Physiology

Table I shows the effect of CA induction on the K_{0.5} (C_i) and V_{max} of photosynthesis for cells grown at both high C_i and low C_i conditions. These data were calculated from the responses shown in Figure 3. For high C_i cells, the kinetic properties before induction appear to be very similar to those of pSK6B, a cell line carrying chloramphenicol resistance but lacking the HCAII gene. Induction of CA expression in these cells leads to a 7-fold increase in the K_{0.5} (C_i) after 2.2 h, a 62-fold increase after 4.8 h, and 152-fold increase after 24 h. During this period there is only a slight reduction in the V_{max}

Table I. Changes in the Kinetic Parameters of Photosynthesis during Induction of CA

Photosynthetic parameters and the accumulation of inorganic carbon were measured as described in "Materials and Methods." The cell suspensions prepared for use in the experiments described in Figure 3 were used for these measurements. Samples of cells were taken at various times after the addition of IPTG as indicated in the table. The final Chl concentrations (μg·mL⁻¹) in the C_i accumulation assays ranged from 19.2 to 22.9 for pCA (1%) cells, 15.2 to 17.0 for pCA (30 ppm) cells, and 20.1 for pSK6B (1%) and 19.4 for pSK6B (30 ppm) cells. For the measurement of photosynthesis, the Chl concentrations in the assays were 2.0 to 5.1 μg·mL⁻¹.

| Cells | Induction Time | V _{max} ^a | K _{0.5} (C _i) | C _i Pool |
|----------------|----------------------|-------------------------------|------------------------------------|---------------------|
| | <i>h</i> | | <i>μM</i> | <i>mM</i> |
| pCA (1%) | 0 | 79 | 125- | 6.4 |
| | 2.2 | 78 | 845 | 2.4 |
| | 4.8 | 70 | 7800 | 0 |
| | 24 | 70 | 19000 | 0 |
| | 24 + EZ ^b | 75 | 650 | |
| pCA (30 ppm) | 0 | 91 | 15 | 8.3 |
| | 1.5 | 89 | 21 | 6.0 |
| | 5 | 76 | 24 | 1.5 |
| | 24 | 56 | 4500 | 0 |
| | 24 + EZ ^c | 63 | 17 | |
| pSK6B (1%) | 0 | 89 | 120 | 20.0 |
| | 4.8 | 91 | 130 | 19.0 |
| pSK6B (30 ppm) | 0 | 102 | 8 | 16.0 |
| | 5.0 | 99 | 6 | 17.0 |

^a μmol O₂·mg⁻¹ Chl·h⁻¹. ^b 50 μM ethoxzolamide was added to the O₂ electrode assays of photosynthetic parameters. ^c 25 μM ethoxzolamide added to assays.

of photosynthesis indicating that expression of CA has specifically altered the affinity of photosynthesis for C_i.

Induction of low-C_i cells results in a similar alteration in cell physiology, but the expression of CA appears to take longer than for 1% CO₂ grown cells. This slower induction during growth at low-C_i is presumably due to the slower rate of growth and protein synthesis under C_i limiting conditions. After 5 h of induction, there was only a slight increase in the K_{0.5} (C_i), but after 24 h there was a dramatic rise to around 4.5 mM, a 300-fold decrease in affinity. There was a significant decrease in the V_{max} of the cells after 24 h induction, indicating that changes other than those affecting the affinity of the cell for external C_i may be occurring. It is possible that when cells are maintained at 30 ppm CO₂ then photoinhibition may occur thus causing a decrease in photosynthetic capacity.

An Increase of Affinity by the Addition of Ethoxzolamide

Ethoxzolamide (EZ) is a potent inhibitor of the HCAII enzyme (11). The K_i for inhibition (1 × 10⁻⁹ M) is some 4 orders of magnitude lower than that measured for the effect of ethoxzolamide on the endogenous CA activity present in extracts from wild-type *Synechococcus* cells (2). It should thus be possible to differentially inhibit the expressed CA activity with low levels of EZ without inhibiting the functions which are performed by the native CA activity as well as the C_i pump (12, 13).

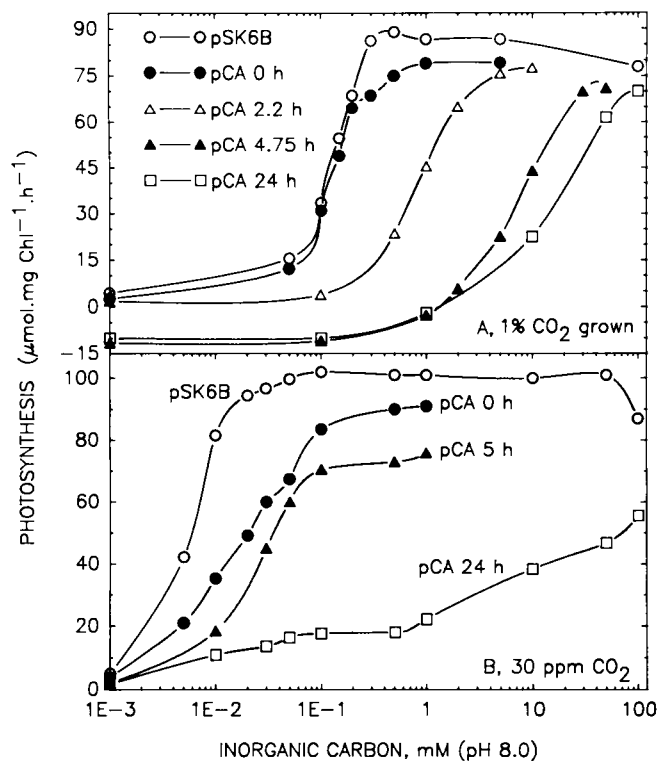


Figure 3. Change in the response of photosynthetic O_2 evolution to external C_i in response to the induction of CA. Cells were taken from the growth tube at the indicated times after the addition of IPTG (0.5 mM) and their response to external C_i was measured. Responses are shown for pCA cells and uninduced pSK6B cells grown at both 1% CO_2 (A) and 30 ppm CO_2 (B). The external C_i is plotted on a logarithmic scale.

The effects of ethoxylamide on the response of photosynthesis to external C_i of induced pCA cells is shown in Figure 4 and the kinetic parameters are reported in Table I. It is clear that the addition of EZ dramatically increases the affinity of the 24 h-induced high- C_i cells for external C_i without altering the V_{max} of photosynthesis. The $K_{0.5}(C_i)$ is not reduced to the same low value as the original uninduced cells but the results are consistent with a reversal of the effect of expressed CA activity on photosynthetic physiology (Fig. 4A). The effect on low C_i cells is even more dramatic with a 260-fold decrease in $K_{0.5}(C_i)$ and a slight increase in V_{max} (Fig. 4b).

Effects of CA Expression on C_i Accumulation

Table I also shows the change in the ability of both low and high- C_i cells to accumulate C_i from the external medium during the induction of CA activity within the cells. Prior to induction, high- C_i cells show a reduced ability to accumulate C_i compared to pSK6B cells. However, the levels of C_i accumulated would appear to be sufficient to support near maximal rates of photosynthesis, as evidenced by the $K_{0.5}(C_i)$ and V_{max} reported in Table I. After 2.2 h of induction, the internal C_i pool is reduced about 3-fold and would be consistent with the increase in the $K_{0.5}(C_i)$ for the same cells (Table I). After 4.8 h, the ability to accumulate is completely abolished and this continues to be the case up to 24 h of induction. The loss

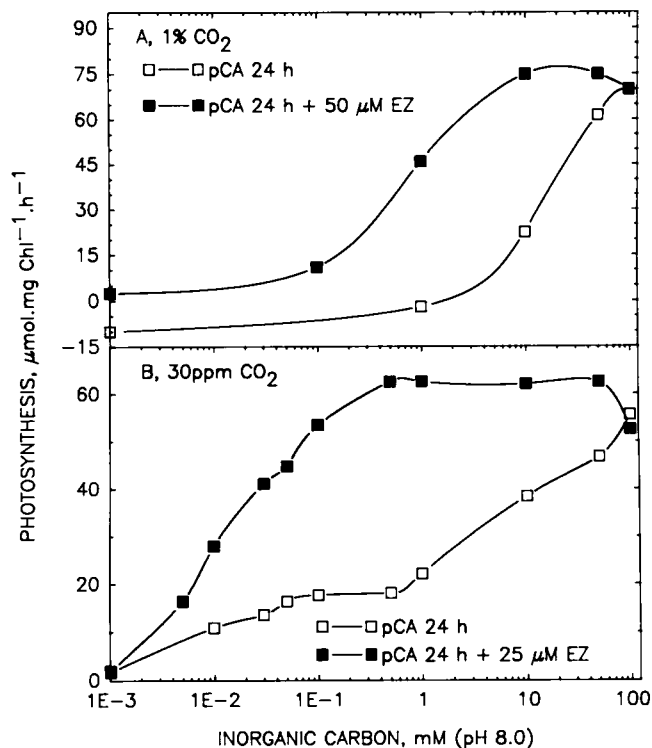


Figure 4. Effect of ethoxylamide on the response of photosynthesis to external C_i after the induction of expression of CA activity in pCA cells. Ethoxylamide was added to assays of both high C_i (A) and low C_i (B) cells which had been induced by the presence of IPTG for 24 h.

of the ability to accumulate C_i correlates well with the dramatic increase in $K_{0.5}(C_i)$.

For low- C_i cells, the changes with induction are quite similar to those seen with high- C_i cells. Prior to the addition of IPTG, the internal C_i pool is again reduced compared to the pSK6B control. After 1.5 h of induction this pool is only slightly decreased and a significant decrease is only seen after 5 h. After 24 h induction, the ability to accumulate C_i is again completely abolished. Thus, the induction of CA under low C_i growth conditions causes a loss of the ability to accumulate C_i but these changes take longer to occur.

Effects of CA Expression on $H^{13}C^{18}O$ Exchange Kinetics

The presence of endogenous CA activity associated with the intact cells has been previously monitored by the use of mass spectrometry to follow the exchange of ^{18}O label out of labeled C_i species into water (2, 3, 18). This has shown that although neither intact high or low C_i cells show externally assayable CA activity, the inorganic carbon which enters the cell undergoes rapid exchange reactions with water which allow the loss of any ^{18}O label present in C_i species. This evidence has been used to infer that CA activity is associated with the cell and may be due to either particulate or soluble forms of CA (2), and may also be a property of the C_i transport mechanism (14). Using this same technique, it is instructive to examine the effects that induced CA activity has on these exchange kinetics.

The exchange kinetics of high- C_i (1%) and low- C_i (30 ppm) cells both before and after 24 h of induction for CA expression are shown in Figures 5 and 6, respectively. The changes following the induction of CA expression are very similar for both growth conditions and are consistent with the synthesis of CA in the cytosol. The depletion of the enrichment (E) when cells are initially injected into the cuvette in the dark is minimal for both uninduced cells and the pSK6B controls. However, after 24 h of induction there is a large and rapid decline in enrichment when pCA cells are injected into the cuvette. This is consistent with the appearance of CA activity in the cytosol, a region which is relatively permeable to CO_2 and relatively impermeable to HCO_3^- .

The changes which are apparent during the light on phase

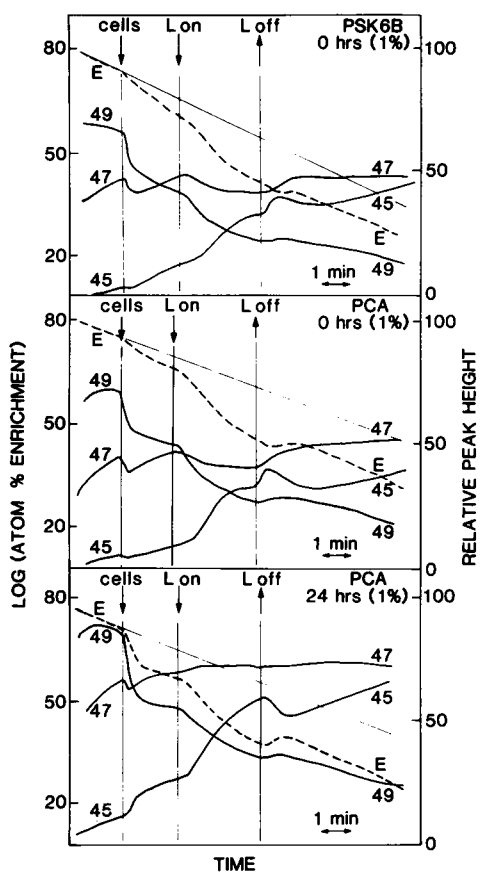


Figure 5. Kinetics of exchange of ^{18}O out of labeled C_i species by 1% CO_2 -grown pCA cells, both before (0 h) and after induction of CA activity by IPTG (24 h). Cells were grown at 1% CO_2 in the presence of chloramphenicol as described in "Materials and Methods." Cells used in these experiments were the same as those prepared for the experiments shown in Figure 3 and Table I. The exchange kinetics of pSK6B cells grown under the same conditions but in the absence of IPTG is also presented as a control. Assays of ^{18}O exchange were performed as described in "Materials and Methods." Assays were initiated by the injection of 300 μL of cell suspension into the darkened cuvette. The response of the peak heights of the labeled CO_2 masses (49, 47, 45) and the atom percent enrichment of doubly labeled CO_2 (E) were recorded for about 2 min prior to switching on the light ($200 \mu mol photons \cdot m^{-2} \cdot s^{-1}$) for a period of 3 min. The final Chl concentrations in the assays were 3.0 (pCA 0), 2.5 (pCA 24), and 2.5 (pSK6B) $\mu gChl \cdot ml^{-1}$.

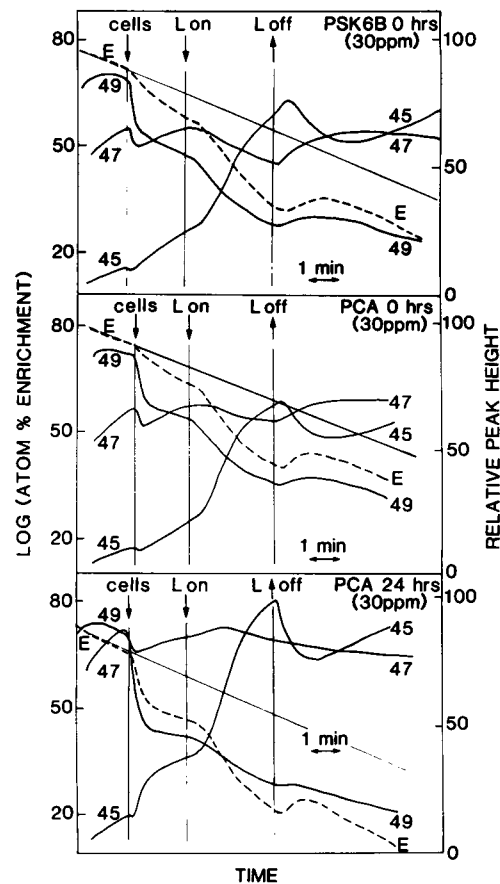


Figure 6. Kinetics of exchange of ^{18}O out of labeled inorganic carbon by 30 ppm-grown pCA cells, both before (0 h) and after (24 h) induction by IPTG. Cells were grown at 30 ppm CO_2 and are the same as those used in the experiments shown in Figure 3 and Table I. The exchange kinetics of pSK6B cells grown under the same conditions is included as a control. The final Chl concentrations of the assays were 4.4 (pCA 0), 4.0 (pCA 24), and 5.2 (pSK6B) $\mu gChl \cdot ml^{-1}$.

are subtle, but are significant in interpreting the effect of the internal CA. In both pSK6B cells and uninduced pCA cells there is a lag in the evolution of unlabeled CO_2 (mass 45) species, following illumination, of about 30 to 40 s in both high and low- C_i grown cells. The lag in the uptake of doubly labeled CO_2 species (49) is much shorter, being about 10 s for low- C_i cells and 18 s for high C_i cells. This would be consistent with the evolution of unlabeled species being dependent on the accumulation of an internal HCO_3^- pool. With 24 h induced pCA cells, the lag in 45 evolution is reduced to around 10 s for low C_i cells and 18 s for high C_i cells. This is consistent with the evolution of unlabeled species occurring immediately the uptake of C_i species has begun without the buildup of an internal C_i pool.

The light off phase shows changes which are indicative of the absence of an accumulated internal C_i pool of induced cells. After darkening in pSK6B and uninduced pCA cells, there is a continuing and increased evolution of unlabeled 45 species for about 30 to 60 s, followed by a decline to a steady state level of increase after 200 to 240 s. This pattern can be interpreted to be due to the cessation of active C_i uptake and

the dissipation of the internal C_i pool via its leakage as CO_2 into the external medium, thus leading to an 'overshoot' in the 45 signal. After 24 h of induction, this overshoot of 45 signal is completely eliminated. As soon as the light is switched off, the 45 signal declines to its steady state rate of increase after about 100 s in the dark. This indicates that there is no accumulated internal pool and subsequently there is a cessation of CO_2 evolution as soon as C_i uptake has stopped.

DISCUSSION

The human carbonic anhydrase II (HCAII) enzyme was expressed in *Synechococcus* PCC7942 by means of transformation with the bidirectional expression vector, pCA. This expression was driven by the bacterial *Tac* promoter and was regulated by the *lacI*Q repressor protein, which was expressed on the same plasmid (Figs. 1 and 2). The level of protein expression reached values of around 0.3% of total cell protein and this protein appeared to be entirely soluble in nature and located within the cytosol of the cell.

The expression of the HCAII enzyme had a dramatic effect on the photosynthetic physiology of the cell, leading to the creation of a high C_i requiring phenotype. Induction of expression of CA activity in both high C_i and low C_i grown cells leads to: (a) a dramatic increase in the $K_{0.5}$ (C_i) for photosynthesis (Table I; Fig. 3) with only a minor effect on the V_{max} , (b) a loss of the ability to accumulate internal C_i (Table I; Figs. 5 and 6), and (c) a decrease in the lag between the initial C_i accumulation following illumination and the efflux of CO_2 from the cells (Figs. 5 and 6). In addition, the effects of the expressed CA can largely be reversed by specific inhibition with ethoxzolamide, indicating that the induction of HCAII is not having other non-specific effects on cell physiology.

As a result of the above findings, it is difficult to conclude otherwise than the CO_2 concentrating mechanism is largely dependent on: (a) the absence of CA activity from the cytosol and (b) the specific localization of CA activity in the carboxysome. This is in direct conflict with earlier assumptions that the CA activity measured in cyanobacteria must be associated with the cytosol (3) and strongly favors a model of photosynthesis in which the carboxysome is of central importance, as has been proposed by Reinhold *et al.* (15). A model of photosynthesis in *Synechococcus* and the role of the carboxysome is shown in Figure 7.

The effect of the expression of CA in pCA cells can be compared to that predicted for the model of Reinhold *et al.* (15). We have taken their model and modified it for the physical parameters which can be estimated for *Synechococcus* PCC7942. The effects of the synthesis of different levels of CA on the expected response of photosynthesis to external C_i is shown in Figure 8. The model data looks qualitatively very similar to the results of the experiments shown in Figure 3. An increase of the cytosolic conversion rate of HCO_3^- to CO_2 of 1,000-fold or more appears to be necessary to achieve the experimentally observed changes in C_i response. Cells induced for 24 h reached a CA level of around 5,000 units per mg Chl (Fig. 2) when activity was measured at 0°C. This translates to about 100,000 units per mL of cytosol volume and will be even greater at 30°C growth conditions. This activity is more than enough to speed up the interconversion

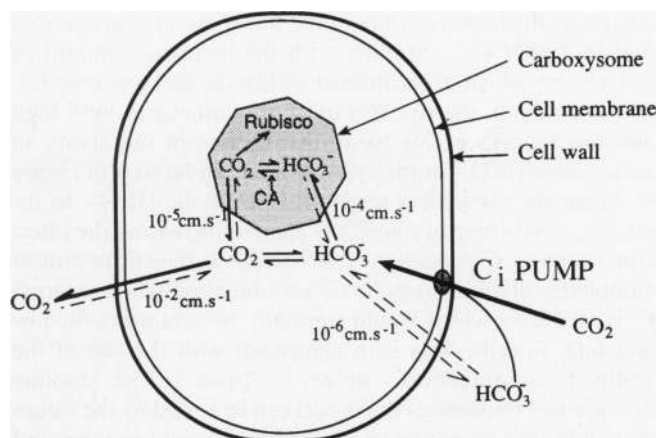


Figure 7. A model of cyanobacterial photosynthesis, incorporating the carboxysome as central location for CO_2 elevation within the cell. The fluxes of CO_2 and HCO_3^- across the cell membrane and carboxysome shell are given the conductances shown and the major direction of the flux is indicated by bold arrows.

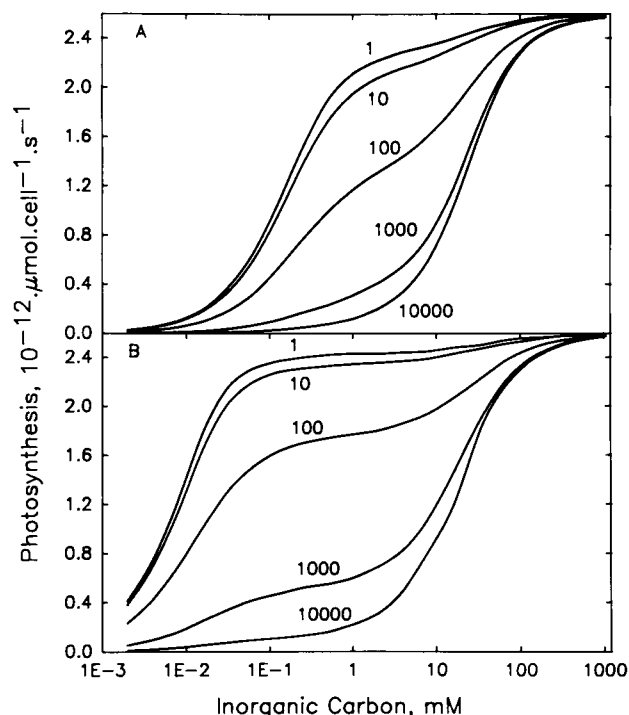


Figure 8. Effect of varying cytosolic CA activity on the theoretical response of photosynthesis in high C_i (A) and low C_i (B) cells to external inorganic carbon. The model is based on the scheme shown in Figure 7 and details of its operation are given in "Materials and Methods." Levels of CA are simulated by increasing the rate constants for the interconversion of CO_2 and HCO_3^- by factors of 10. A rate of photosynthesis of $2.4 \times 10^{-12} \mu\text{mol} \cdot \text{cell}^{-1} \cdot \text{s}^{-1}$ is equal to $278 \mu\text{mol} \cdot \text{mg Chl}^{-1} \cdot \text{h}^{-1}$.

of C_i species by at least 1,000-fold. The data for low C_i cells show some interesting similarities to the modeled response. At low external C_i concentrations, in both the data and the model, there is less reduction in photosynthesis than is seen for high C_i cells. This is due to two elements in the model,

one being the higher affinity of the transporter for external C_i and its higher V_{max} , together with the increased amount of CA activity which is partitioned within the carboxysome (2). The decrease in the $K_{0.5}$ (C_i) of photosynthesis in both high and low C_i cells is due to an elimination of the ability to accumulate HCO_3^- in the cytosol. This can be seen in Figure 9, where the theoretical response of cytosolic HCO_3^- to increasing levels of cytosolic CA is shown. Increasing the interconversion of C_i species by 1,000-fold is sufficient to almost completely abolish cytosolic C_i accumulation when external C_i is at a level which would normally be saturating for low and high C_i cells. This is in agreement with the loss of the ability to accumulate C_i shown in Table I. The absolute quantitative response of the model can be varied by the values chosen for the properties of the pump, the conductances and the CA levels, but the agreement seen here strongly supports a model of photosynthesis which attributes a central role to the carboxysome as shown in Figure 7.

To function as the site for CO_2 concentration in the cyanobacterial cell, the carboxysome must be proposed to have certain special physical properties. One of these is obviously a localization of both Rubisco and CA activity within its structure. A second and perhaps more essential feature which is absolutely required is the presence of a mechanism to reduce the leak rate of CO_2 out of the carboxysome.

Two mechanisms have been proposed by Reinhold *et al.* (15) to achieve a reduction in the leak rate for CO_2 . First, the protein monolayer shell which surrounds the carboxysome may have special diffusive properties which impede the movement of nonpolar gaseous molecules such as CO_2 and O_2 , while permitting a more rapid entry of ionic substrates such as RuP_2 and HCO_3^- than would be allowed by a lipid bilayer membrane. The properties of such membranes to the movement of ionic species is not known but in general, the properties of a hydrophilic protein coat should be much more polar in nature and this should act to essentially 'salt out' nonpolar gases from the water contained in the membrane,

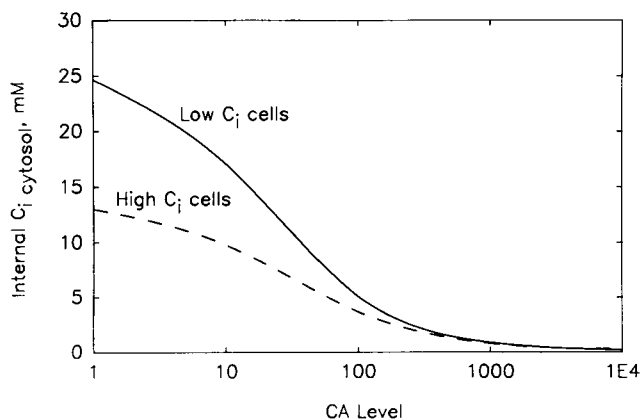


Figure 9. Theoretical effect of increasing CA level on the cytosolic HCO_3^- pool in high and low C_i cells, when the external C_i is maintained at 1 and 0.1 mM, respectively. Details of the model from which the data were calculated are given under Figure 8, and increasing CA in the cytosol was simulated by multiplying the rate constants for the interconversion of CO_2 and HCO_3^- from 1 to 10,000-fold. Note that the CA axis is logarithmic.

while permitting the diffusion of ionic species at a rate which would be significantly enhanced compared to a lipid bilayer.

The second mechanism proposed to reduce the leak would be to localize the carbonic anhydrase to a position at the center of the carboxysome, thus surrounding it by a shell of Rubisco molecules (15). In this case, the initial generation of CO_2 would occur at the center of the carboxysome and the CO_2 would be forced to diffuse outward through the Rubisco molecules. This could act to produce a gradient of CO_2 concentration from the center to the outside. This would reduce the final CO_2 gradient which would exist across the interface between the carboxysome and the cytosol and thus decrease the potential leak rate. Whether such a mechanism could act by itself to sufficiently reduce the leak or if it could only be seen as an adjunct to an external diffusion barrier is unknown.

Some direct physical evidence that the carboxysome may have the properties necessary to perform this central role in cyanobacterial photosynthesis is available. Rubisco activity has been shown to be intimately associated with carboxysomes and recently it has been found the CA activity in *Synechococcus* PCC7942 is largely associated with a particulate fraction which correlates with the carboxysome fraction of the cell (2).

The characterisation of the diffusive properties of the carboxysome have been less rewarding and results have been conflicting. Coleman *et al.* (5) initially reported that Rubisco activity association with the carboxysomes of *Coccochloris pennicystis* was largely insensitive to oxygen. From this they inferred that the protein monolayer encapsulating the carboxysome may have special properties which impede the diffusion of gaseous nonpolar species while permitting the passage of ionic molecules. Unfortunately, it has not been possible to duplicate these results with other species (MR Badger, GD Price, unpublished data) or to our knowledge with *Coccochloris*, so some doubt must exist as to whether this is a general property of carboxysomes. Considering the above models, it would be expected that it should be possible to measure a diffusive barrier for CO_2 to the site carboxylation in carboxysomes and that HCO_3^- would act as a preferential substrate. In addition, the inhibition of carbonic anhydrase by ethoxazolamide should alter the response of carboxysomal Rubisco to external C_i . Unfortunately, specific experiments designed by us to test these properties have proved negative (MR Badger, GD Price, unpublished results) and it remains to be shown if isolated carboxysomes can be shown to have the properties which are consistent with their apparent role in the cell. However, it can always be argued that damage occurs to the protein coat during extraction and it is not possible to emulate the *in vivo* physiology.

The findings presented in this paper allow a number of clear statements to be made about various aspects of the operation of the CO_2 concentrating mechanism in cyanobacteria and these are summarised in the model presented in Figure 7. Several aspects of functioning which have been open to speculation can now be resolved with a much higher degree of certainty:

(a) The resistance to CO_2 leakage from the cell must reside at the level of the carboxysome and not the cell membrane, as had previously been proposed (3).

(b) Inorganic carbon which is pumped into the cell must arrive in the form of HCO_3^- rather than CO_2 for the carboxysome model to function. This supports the model of the C_i transport mechanism proposed recently by Price and Badger (13) for both high and low C_i cells in which the pump is proposed to have CA-like properties and is able to transport CO_2 as the primary species from the external medium and convert it to HCO_3^- which is released inside the cell.

(c) Carbonic anhydrase is absent from the cytosol and is localised within the carboxysome.

(d) The Rubisco which is localised within the carboxysome is the only form of the enzyme which can be used by the cell for photosynthesis. Previous speculation that carboxysomal Rubisco may be a storage form of the enzyme (4) appears to be false. If the carboxysomal model of photosynthesis is correct, then a cytosolic form of the enzyme would be largely inactive due to the low CO_2 present in the cytosol, except in environments where the external CO_2 rose to levels which would act as a substrate for the cytosolic enzyme.

While the scenario which we have concluded in this paper is most compelling, we are concerned at the lack of complete physical evidence that the carboxysome possesses the properties necessary to achieve its apparent function. Further research in this area is necessary, and it will be important to discover the basis for the CO_2 leak barrier associated with this polyhedral body.

It is interesting to speculate on whether the functional role of the carboxysome may be emulated in any other aquatic phototroph which is proposed to possess a CO_2 concentrating mechanism. The elementary functional elements which would need to be present would presumably be the localization of Rubisco and CA activity in some membrane-bound structure. One particular body which could fulfill this role is the pyrenoid in green algae. This body has been shown to contain Rubisco protein and its role has not been clearly established (9). No special attempt has been made to examine the activity of CA in this body but it is possible that CO_2 elevation may occur here. Further work is necessary to explore this possibility.

ACKNOWLEDGMENTS

We would like to thank Professor S. Lindskog and Dr. B-H. Jonsson for kindly making available to us the pHCAII vector. In addition, we thank Dr. M. K. Morell for the gene base search which directed us to obtaining the above vector and to Ms. Susan Kirby for her expert technical assistance.

LITERATURE CITED

1. **Badger MR** (1987) The CO_2 concentrating mechanism in aquatic phototrophs. In MD Hatch, NK Boardman, eds. *The Biochemistry of Plants: A Comprehensive Treatise*. Vol. 10, Photosynthesis. Academic Press, New York, pp 219–274
2. **Badger MR, Price GD** (1989) Carbonic anhydrase associated with the cyanobacterium *Synechococcus* PCC7942. *Plant Physiol* **89**: 51–60
3. **Badger MR, Bassett M, Comins HN** (1985) A model for HCO_3^- accumulation and photosynthesis in the cyanobacterium *Synechococcus* sp. *Plant Physiol* **77**: 465–471
4. **Codd GA, Marsden WJN** (1984) The carboxysomes (polyhedral bodies) of autotrophic prokaryotes. *Biol Rev* **59**: 389–422
5. **Coleman JR, Seemann JR, Berry JA** (1982) RuBP carboxylase in carboxysomes of blue-green algae. *Carnegie Inst Wash Year Book* **81**: 83–87
6. **Dzelzkalns VA, Owens GC, Bogorad L** (1984) Chloroplast promoter driven expression of the chloramphenicol acetyl transferase gene in a cyanobacterium. *Nucleic Acids Res* **12**: 8917–8925
7. **Forsman C, Behrven G, Osterman A, Jonsson B-H** (1988) Production of active human carbonic anhydrase II in *E. coli*. *Acta Chem Scand* **B42**: 314–318
8. **Golden SS, Busslan J, Haselkorn R** (1987) Genetic engineering of the cyanobacterial chromosome. *Methods Enzymol* **153**: 215–231
9. **Holdsworth RH** (1971) The isolation and the partial characterization of the pyrenoid protein from *Eremosphaera viridis*. *J Cell Biol* **15**: 499–513
10. **Maniatis T, Fritsch EF, Sambrook J** (1982) *Molecular Cloning. A Laboratory Manual*. Cold Spring Harbor Laboratory, Cold Spring Harbor, NY
11. **Maren TH** (1984) The general physiology of reactions catalyzed by carbonic anhydrases and their inhibition by sulphonamides. *Ann NY Acad Sci* **429**: 568–579
12. **Price GD, Badger MR** (1989) Ethoxycarbonyl inhibition of CO_2 -dependent photosynthesis in the cyanobacterium *Synechococcus* PCC7942. *Plant Physiol* **89**: 44–50
13. **Price GD, Badger MR** (1989) Ethoxycarbonyl inhibition of CO_2 uptake in the cyanobacterium *Synechococcus* PCC7942 without apparent inhibition of internal carbonic anhydrase activity. *Plant Physiol* **89**: 37–43
14. **Price GD, Badger MR** (1989) Isolation and characterization of high- CO_2 requiring mutants of the cyanobacterium *Synechococcus* PCC 7942: two phenotypes that accumulate inorganic carbon but are unable to generate CO_2 within the carboxysome. *Plant Physiol* **91**: 514–525
15. **Reinhold L, Zviman M, Kaplan A** (1987) Inorganic carbon fluxes and photosynthesis in cyanobacteria—a quantitative model. In J Biggins, ed, *Progress in Photosynthesis*, Vol IV. Martinus Nijhoff, Dordrecht, Netherlands, pp 6.289–6.296
16. **Rickli EE, Ghanzafar SAS, Gibbons BH, Edsall JT** (1964) Carbonic anhydrase from human erythrocytes. *J Biol Chem* **239**: 1065–1075
17. **Ripka R, Waterbury JB, Stanier RY** (1981) Isolation and purification of cyanobacteria: Some General Principles. In MP Staff, H Stolp, HG Truper, A Balows, HG Schlegel, eds, *The Prokaryotes*. Springer-Verlag, Berlin, pp 212–220
18. **Tu CK, Avecedo-Duncan M, Wynns CG, Silverman DN** (1986) Oxygen-18 exchange as a measure of the accessibility of CO_2 and HCO_3^- to carbonic anhydrase in *Chlorella vulgaris* (UTEX 263). *Plant Physiol* **85**: 72–77
19. **Wilbur KM, Anderson NG** (1948) Electrometric and colorimetric determination of carbonic anhydrase. *J Biol Chem* **176**: 147–154
20. **Wintermans JFGM, de Mots A** (1965) Spectrophotometric characteristics of chlorophylls a and b and their pheophytins in ethanol. *Biochim Biophys Acta* **109**: 448–453
21. **Yanisch-Perron C, Vieira J, Messing J** (1985) Improved M13 phage cloning vectors and host strains: Nucleotide sequences of the M13mp18 and pUC19 vectors. *Gene* **33**: 103–119